Journal of Sound and Vibration (2001) **246**(5), 815–827
doi:10.1006/jsvi.2001.3653, available online at http://www.idealibrary.com on IDEAL®

DAMPING ESTIMATES FROM EXPERIMENTAL NON-LINEAR TIME-SERIES

J. M. Nichols, L. N. Virgin and H. P. Gavin

Pratt School of Engineering, Duke University, NC 27708-0300, *U.S.A.*

(*Received* 15 *May* 2000, *and in final form* 5 *February* 2001)

This paper seeks to illustrate the utility of the Lyapunov spectrum in estimating the damping of an experimental non-linear system. A mechanical model of Duffing's equation operating in the chaotic regime is used to generate a single observable. Using standard techniques from non-linear time-series analysis, the complete Lyapunov spectrum is estimated. The sum of these exponents may, via the divergence theorem, be related directly to the coefficient of viscous damping. Estimations are performed in this manner for both a three- and four-dimensional response and results are compared to estimates taken from two linear-based techniques. The indication is that use of the Lyapunov spectrum to obtain quantitative damping estimates is a comparable alternative to methods requiring transient data or detailed knowledge of the dynamics.

1. INTRODUCTION

One of the more difficult tasks involved in modelling non-linear mechanical systems is the estimation of the parameter(s) involved in energy dissipation. Even in the case of a simple viscous damping model, it is often challenging to extract the relevant constant of proportionality from experimental data. Traditionally, linear system identification tools such as the logarithmic decrement (log-dec), global parameter fitting [1], and various frequency domain techniques [2] have been used for this purpose. Many of these techniques involve observing a transient response, or require that the underlying equations of motion be known. In certain instances, this information may not be available, especially if the system in question is operating in a non-linear, possibly chaotic, regime. The aim of this paper is to show that accurate damping estimations may be acquired without either (1) observing the unforced (transient) response or (2) knowing the form of the non-linearity.

Shin and Hammond [3] showed that the sum of a system's Lyapunov exponents (LEs) could provide an insight into the damping mechanisms present in the system. Specifically, they were able to show that the sum of the LEs may be related to the system's divergence. In the instance of viscous (time invariant) damping the divergence, hence the sum of the LEs, is in fact equal to the coefficient of viscous damping. Since Lyapunov spectrum estimations are possible from chaotic data, the system in question is not restricted to transient response. Furthermore, if the non-linearity is in the "stiffness" term, the actual *form* of the non-linearity is unimportant. In this work, an experimental model of the forced Duffing oscillator with viscous damping is considered. This particular system has been well studied, both experimentally and numerically [4, 5], and its invariant properties are well known making it an ideal model to study. The coefficient of viscous damping is estimated directly

0022-460X/01/400815 + 13 $35.00/0

from an experimental chaotic time history and results compared to those obtained from two other approaches, the logarithmic decrement and a global parameter fitting scheme. Results are also obtained from the two frequency forced Duffing oscillator. The effect of adding the second forcing term is to increase the dimensionality of the response by one.

2. LYAPUNOV SPECTRUM AND THE DIVERGENCE THEOREM

Assume a dynamical system which obeys

$$\dot{\mathbf{x}}(t) = \mathbf{F}(\mathbf{x}(t)). \tag{1}$$

The state of the system at any point in time is specified by the vector $\mathbf{x}(t)$ whose components define a basis referred to as the principal axes. An ensemble of trajectories evolve in time as a flow, tracing out a dynamical attractor in the state space as $t \to \infty$. The Lyapunov spectrum defines the exponential rate at which perturbations to the system diverge or converge in each of the principal directions. Letting $P_i(t)$ govern the evolution of an infinitesimal perturbation to a trajectory along the ith principal axis, the complete spectrum of Lyapunov exponents (LEs) may be written as

$$\lambda_i = \lim_{t \to \infty} \frac{1}{t} \ln \frac{P_i(t)}{P_i(0)} \quad i \in 1 \cdots d, \tag{2}$$

where d is the dimension of the system. Alternatively, equation (2) may be thought of as the average rate at which the axes of an infinitesimal, d-dimensional hyper-sphere of volume $V(0) = \prod_i^d P_i(0)$ deform under the action of the flow. In terms of volume elements, we may write

$$V(t) = V(0) \mathrm{e}^{(\lambda_1 + \lambda_2 + \cdots + \lambda_d)t}. \tag{3}$$

Equation (3) simply states that, on average, the volume of the state space will evolve as the sum of the LEs.

Shin and Hammond [3] noted that the divergence of a flow also provides information related to the time evolution of small volume elements. For systems governed by equation (1), the divergence is written [6] as

$$\nabla(\dot{\mathbf{x}}(t)) = \sum_i \partial F_i / \partial x_i|_t. \tag{4}$$

This quantity may be related to the *local* evolution of a small volume element in state space via

$$\frac{1}{V(t)} \dot{V}(t) = \nabla(\dot{\mathbf{x}}(t)), \tag{5}$$

the solution of which resembles equation (3) with the divergence replacing the sum of the LEs in the exponential. The divergence is time varying and depends on the location on the flow at which it is evaluated. The Lyapunov spectrum, however, is an invariant property of the system representing *global* system properties. Relating the two quantities therefore requires defining an *instantaneous* Lyapunov exponent (ILE). In order to further the

development, equation (2) may be rewritten in discrete time using the chain rule as

$$\lambda_i = \lim_{N\to\infty} \frac{1}{N} \ln\left(\prod_{n=0}^{N} \frac{P_i(n+1)}{P_i(n)}\right) \tag{6}$$

$$= \lim_{N\to\infty} \frac{1}{N}\left(\sum_{n=0}^{N} \ln\left(\frac{P_i(n+1)}{P_i(n)}\right)\right), \tag{7}$$

where the switch has been made to discrete time using $t = N\Delta t$ and Δt^{-1} is the sampling rate. By defining a local or instantaneous Lyapunov exponent,

$$\hat{\lambda}_i(n) = \ln \frac{P_i(n+1)}{P_i(n)}, \tag{8}$$

the global measure simply becomes the time average of the local quantities. It is these local exponents that govern the expansion/contraction of the flow over short times. Following the development of Shin and Hammond, we may finally write

$$\nabla(\dot{\mathbf{x}}(n)) = \sum_{i=1}^{d} \hat{\lambda}_i(n) \tag{9}$$

so that the divergence of the flow is equal to the sum of the ILEs at any point on the flow. We may cast the problem into a more practical form by rewriting equation (6) in terms of the Jacobian of the flow as

$$\lambda_i = \lim_{N\to\infty} \frac{1}{N} \ln\left|\mathrm{eig}_i\left(\prod_{n=0}^{N} \mathbf{J}(\mathbf{x}(n))\right)\right|, \quad i = 1 \cdots d, \tag{10}$$

where we have made use of the fact that in the local linear approximation,

$$\begin{Bmatrix} P_1(n+1) \\ P_2(n+1) \\ \vdots \\ P_i(n+1) \end{Bmatrix} = \mathbf{J}(\mathbf{x}(n)) \begin{Bmatrix} P_1(n) \\ P_2(n) \\ \vdots \\ P_i(n) \end{Bmatrix}. \tag{11}$$

The exponential expansion/contraction of perturbations are therefore governed by the d eigenvalues (eig_i) of the product of N local Jacobians. It is this form of equation (2) which most easily lends itself to both analytic and numeric calculations.

As an example, consider a form of the forced linear oscillator with viscous damping

$$\dot{X}_1 = X_2, \qquad \dot{X}_2 = -2\zeta\omega_n X_2 - \omega_n^2 X_1 + A\sin(X_3), \qquad \dot{X}_3 = \omega. \tag{12}$$

The divergence for this flow is simply the quantity preceding X_2 in the second state equation. Therefore, the sum of the ILEs for this system should be equal to $-2\zeta\omega_n$. The Lyapunov spectrum may be computed analytically by first forming the Jacobian

$$\mathbf{J} = \begin{pmatrix} 0 & 1 & 0 \\ -\omega_n^2 & -2\zeta\omega_n & A\cos(X_3) \\ 0 & 0 & 0 \end{pmatrix}. \tag{13}$$

This Jacobian has a single zero eigenvalue associated with the third row/column ($\text{eig}_1 = 0$) and two non-zero eigenvalues associated with the upper left 2 by 2 block of **J**. This submatrix is time invariant so that

$$\ln\left|\text{eig}_{2,3}\left(\prod_{n=0}^{N}\mathbf{J}(\mathbf{x}(n))\right)\right| = \ln|\text{eig}_{2,3}(\mathbf{J}(\mathbf{x}(n)))| \tag{14}$$

$$= \text{Re}\{-\zeta\omega_n \pm i\omega_n\sqrt{1-\zeta^2}\}, \tag{15}$$

where we have assumed an underdamped system (i.e., $\zeta < 1$). Therefore, the non-zero Lyapunov exponents for this system are simply the real parts of the characteristic exponents [7]. The complete spectrum for this oscillator is: $\lambda_1 = 0{\cdot}0$, (corresponding to the 'time' direction) $\lambda_2 = \lambda_3 = -\zeta\omega_n$ so that the sum is $-2\zeta\omega_n$ as predicted by the divergence theorem. This type of analysis typically lends itself only to linear systems. For a chaotic system (i.e., where one of the $\lambda_i > 0{\cdot}0$), each of the N Jacobians must be computed and their eigenvalues extracted in turn.

2.1. SPECTRUM ESTIMATION

The implementation of equation (10) involves estimating successive Jacobians, **J**, at a specific trajectory, $\mathbf{x}(n)$, as it winds its way around the attractor. The eigenvalues of these Jacobians may then be computed and averaged over the number of estimations made. For systems obeying an underlying analytical model, the computations are simple because the Jacobian is known at any point on the flow (see Wolf [8]). However, if the equations of motion are not known *a priori* the task becomes more involved.

Several algorithms exist for extracting the complete Lyapunov spectrum from a scalar time-series. In each, the critical first step is to reconstruct the dynamical attractor from the time-series measure. Rather than use the familiar delay co-ordinates [9], we employ the algorithm of Darbyshire and Broomhead [10] in which the reconstruction is based on principal component analysis. This particular method has the advantage of eliminating much of the additive noise which often accompanies experimental measurement. The computations of LEs may become distorted for noise levels as low as 1% [10] making it essential that the noise floor be reduced. The method proceeds by embedding the system into a high-dimensional space with a delay of one time step. The resulting vectors, constructed from an observable x at discrete time n, may be written as

$$\mathbf{x}(n) = (x(n), x(n+1), x(n+2), \ldots, x(n+(d_w-1))). \tag{16}$$

Row by row, these vectors make up the *trajectory* or Hankel [11] matrix, **X**, which may be thought of as containing all the patterns present in the data for large enough window length, d_w. Typical values for a reasonably sampled system are $20 \leqslant d_w \leqslant 80$. For a more thorough discussion of the effects of window length on the resulting computations, see reference [12].

The next step is to compute the singular value decomposition (SVD) of **X** into its right and left singular vectors and their associated singular values

$$\mathbf{X} = \mathbf{U}\mathbf{\Sigma}\mathbf{V}^{\mathrm{T}}. \tag{17}$$

The left singular vectors, **U**, represent a new basis in d_w space, chosen such that it spans most of the data in a least-squares sense. The associated singular values given by the

diagonal entries of $\mathbf{\Sigma}$ relate the degree to which the data spans this new space. These singular values are given in decreasing order so that the most heavily populated directions are given by the first few columns of $\mathbf{U}$. The final step is to project $\mathbf{X}$ onto the d_e directions associated with the largest singular values

$$\hat{\mathbf{X}} = \mathbf{X}\hat{\mathbf{U}}, \tag{18}$$

where $\hat{\mathbf{U}}$ simply consists of the first d_e columns of $\mathbf{U}$ and d_e will be referred to as the embedding dimension. The remaining $d_w - d_e$ directions are assumed to contain noise and are discarded. This method of embedding therefore has two distinct advantages over time delay embedding. Not only is the choice of delay eliminated from the embedding process, but the data is filtered as well. However, as has been pointed out by Grassberger *et al.* [13], the filtering aspect may not be "a good general-purpose noise reduction scheme, as it just corresponds to linear filtering". Still, the method has been widely used in practice [14, 15] for the purposes of noise reduction in attractor reconstruction.

The question of how to choose the d_e sub-space on which the data is projected is easily addressed. Past literature has focused on using a generalization of Whitney's embedding theorem [16] where $d_e > 2D_f$ and D_f is the fractal dimension of the attractor. While sufficient, this criteria is not necessary as many dynamical systems may be embedded in fewer dimensions. We prefer to use the empirical method outlined by Kennel and Abarbanel [17] where the goal is to eliminate all false projections of the data caused by embedding in too small a space. By setting a threshold for what constitutes a falsely projected pair of neighbors, the data are embedded into successively higher dimensions until no pairs of neighbors are near due to projection, but rather due only to the geometry of the attractor.

The reconstructed attractor is now given by $\hat{\mathbf{X}}$ whose rows are simply the pseudo state vectors at a given point in time. For the discussion that follows, the hat ($\hat{}$) is dropped for notational convenience so that individual trajectories are simply given by $\mathbf{x}(n)$. From the attractor, a main, or *fiducial*, trajectory $\mathbf{x}_f(n)$ is selected to serve as the basis for subsequent calculations. Perturbation vectors to the system at discrete time n are approximated by

$$\mathbf{y}_i(n) = \mathbf{x}_i(p) - \mathbf{x}_f(n) \quad i \in 1 \cdots N_b, \tag{19}$$

where the $\mathbf{x}_i(p)$ are the nearest N_b trajectories to the fiducial trajectory in a Euclidean sense. Note that the index p need not be related in time to the index of the fiducial trajectory n. The perturbations are allowed to evolve some small time Δ into the future giving

$$\mathbf{y}_i^+(n + \Delta) = \mathbf{x}_i(p + \Delta) - \mathbf{x}_f(n + \Delta). \tag{20}$$

Both the initial and final sets of perturbation vectors are used, row by row, to form the perturbation matrices $\mathbf{Y}$ and $\mathbf{Y}^+$. The key relation governing the time evolution of the perturbations is simply

$$\mathbf{Y}^+ = \mathbf{J}(\mathbf{x}_f(n))\mathbf{Y}, \tag{21}$$

where the mapping $\mathbf{J}(\mathbf{x}_f(n))$ is the quantity to be computed. Often, $\mathbf{J}(\mathbf{x}_f(n))$ is estimated by using a least-squares fit for a given set of basis functions (e.g., polynomial) and the linear term retained as the Jacobian (see references [18] or [19]). However, we employ the pseudo-inverse method advocated by Broomhead [10] in which the Jacobian is computed directly. For the systems we have studied, this method gives improved estimates of the dominant negative exponent over those obtained from a least-squares polynomial fit. The final step is to extract the eigenvalues using QR decomposition [20]. Taking $\mathbf{Q}_0 = \mathbf{I}$, where

I is the identity matrix, the QR procedure may be written as

$$\mathbf{J}_n\mathbf{Q}_{n-1} = \mathbf{Q}_n\mathbf{R}_n, \tag{22}$$

for the nth Jacobian. The matrix $\mathbf{Q}_n$ contains the basis for the subsequent calculation while the diagonal entries of $\mathbf{R}_n$ contain the desired eigenvalues. The calculation is recursive for each of the N Jacobians as they are estimated. Using this procedure, equation (10) may be rewritten in practice as

$$\lambda_i = \frac{1}{N}\sum_{n=1}^{N} \ln(\mathbf{R}_n)_{ii}, \tag{23}$$

where λ_i are the global Lyapunov exponents and $(\mathbf{R}_n)_{ii}$ are the eigenvalues of $\mathbf{J}_n$ given by the diagonal entries of $\mathbf{R}_n$. The goal then, is to repeat the above process for as many local neighborhoods as possible as $\mathbf{x}_f(n)$ advances through the data set.

2.2. KAPLAN–YORKE CONJECTURE

There exists a check between fractal dimension and Lyapunov spectrum which may increase confidence in results. The Kaplan–Yorke conjecture states that the fractal dimension of the attractor in question may be related to its Lyapunov spectrum through

$$D_L = k + \frac{\sum_{m=1}^{k}\lambda_m}{-\lambda_{k+1}}, \tag{24}$$

where the parameter k is the maximum number of Lyapunov exponents which can be added together before the sum becomes negative. The resulting measure, D_L, is typically close, if not equal to, the value for the correlation dimension (d_c) [18, 19]. Computations of d_c may therefore be used as a check against the spectrum values.

3. APPLICATION

The model under study is a modified form of the Duffing system given by

$$\dot{X}_1 = X_2, \qquad \dot{X}_2 = -2\zeta X_2 + \frac{1}{2}(X_1 - X_1^3) + F_1\Omega_1^2\sin(X_3) + F_2\Omega_2^2\sin(X_4),$$

$$\dot{X}_3 = \Omega_1, \qquad \dot{X}_4 = \Omega_2. \tag{25}$$

With appropriately chosen parameters, it has been shown [21] that these equations approximate the motion of a cart rolling on a two-well potential surface subject to base excitation. The state variables X_1, X_2 may be thought of as the relative position and velocity of the cart with respect to the surface, while X_3, X_4 represent the angular displacement of the forcing. Forcing is a superposition of two sinusoids with constant amplitudes F_1, F_2 and angular frequencies Ω_1, Ω_2, while damping is approximated by a viscous model with damping ratio ζ. Having two frequencies is a convenient method of altering the dimension of the system in an experimental context without altering the damping. The cart position has been non-dimensionalized so that stable equilibria occur at $X_1^{(e)} = \pm 1$. Application of the divergence theorem to this system in either case (single or

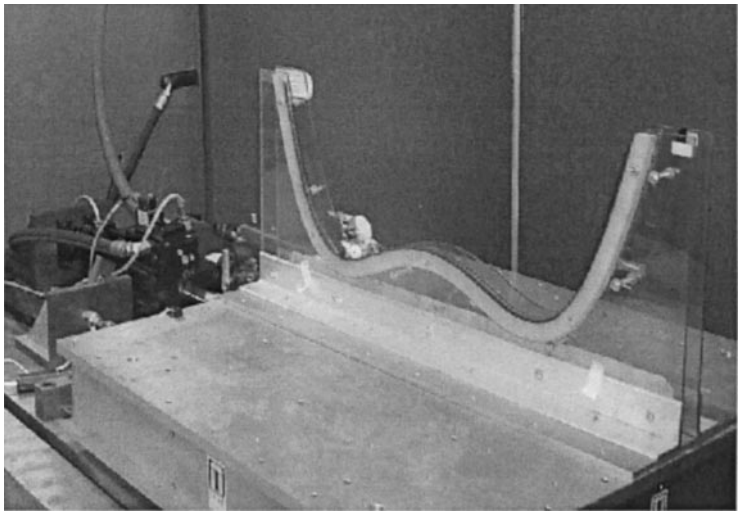

Figure 1. Experimental setup.

two-frequency forcing) provides the same result as for the simple mechanical oscillator. The divergence of this non-linear flow is -2ζ, so that the sum of the systems local Lyapunov exponents should give a direct estimate of the damping. Since the divergence is constant in time, this is a special case of equation (9) in which the *global* LEs will be equal to the divergence of the flow.

The experimental setup is shown in Figure 1 and consists of the cart/track apparatus mounted on a 1·2 m by 1·2 m hydraulically actuated shaker table. Forcing is generated digitally and transformed into base motion via a PIDF digital controller. The cart position was recorded by means of a potentiometer while the base position was monitored using an LVDT sensor. Further details of this experimental testbed can be found in reference [4].

3.1. RESULTS

Two cases were considered for application of the divergence theorem. In the first, $F_1 = 0{\cdot}19$ (5·08 cm), $F_2 = 0$ and $\Omega_1 = 0{\cdot}84$ (1 Hz) so that equations (25) reduce to a three-dimensional system with single frequency forcing. The second case involves setting $F_2 = F_1 = 0{\cdot}141$ (3·81 cm.), $\Omega_1 = 0{\cdot}84$, and requiring that Ω_1/Ω_2 be an irrational number (specifically the fractional part of the golden mean), effectively increasing the dimensionality of the system by one. In both instances, the measured quantity was the position, X_1, and consisted of 50 000 observations sampled at $\tau_s = 0{\cdot}01$ s.

Attractor reconstruction was performed by using the SVD embedding of section 2.1 with a window length of $d_w = 50$. The computation of d_e for both the single and two-frequency forced cases are illustrated in Figure 2(a) and 2(b). A global embedding of $d_e = 4$ dimensions is clearly needed in order to eliminate false projections for both the single- and two-frequency forced cases. The next question to address is that of a *local* or dynamical dimension. The local dimension, d_l, refers to the number of dynamical variables in a system and hence the number of LEs. Due to curvature, many systems 'live' in a global space which exceeds the number of degrees of freedom. Since the neighborhoods in the estimation procedure are chosen in d_e there will be $d_e - d_l$ spurious exponents. For example, in the case of single-frequency forcing, the analytic model clearly predicts three degrees of freedom yet

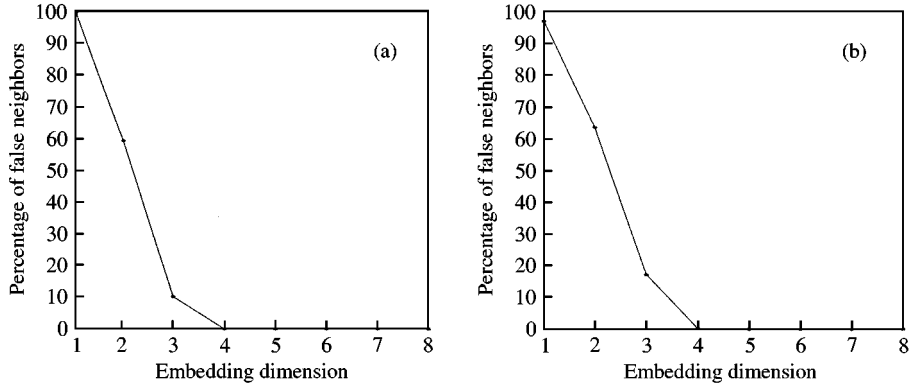

Figure. 2. Global embedding for (a) single and (b) two-frequency forced system.

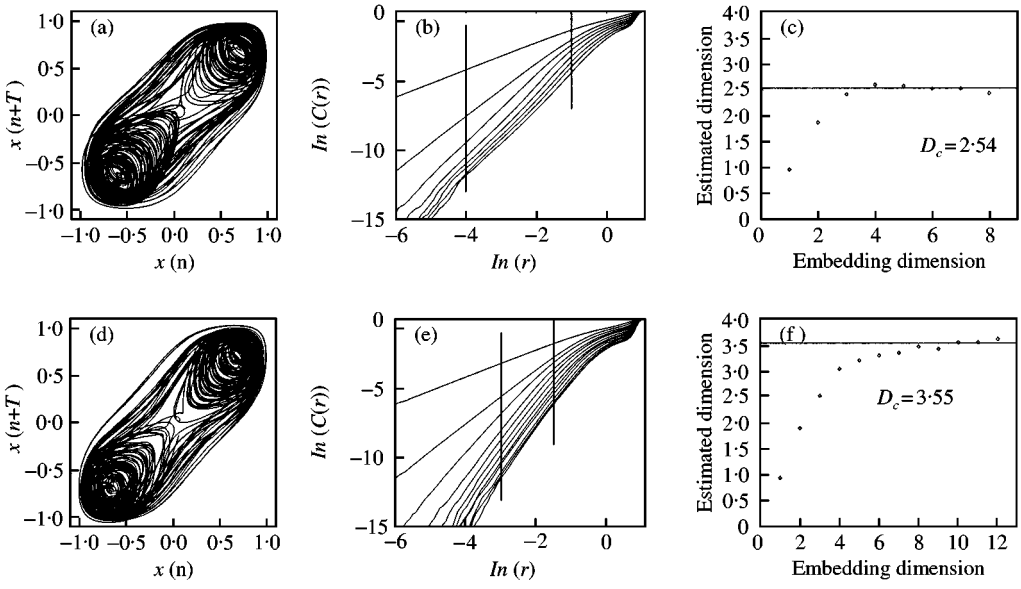

Figure 3. Correlation dimension for single (top row) and two frequency (bottom row) forced systems. Shown here are the (a, d) attractors, (b, e) correlation sum, and (c, f) progression of slope with embedding.

the attractor lives in four-dimensional space. Two methods currently exist that we are aware of for quantifying the local dimension of a chaotic system. The first is to simply compute the correlation dimension for the system and use $d_l = \text{ceil}(d_c)$ where the 'ceil' operator simply rounds d_c up to the nearest integer. Another method proposed by Abarbanel and Kennel [22] also estimates this quantity, however, for attractors with high degrees of curvature, the method produced poor results. Representative results from the computation of d_c are shown in Figure 3. Plots 3(a, d) illustrate the reconstructed attractors based on a delay co-ordinate reconstruction with $T = 24$ timesteps (found through mutual information). Scaling regions were chosen based on the local slope of plots 3(b, e) and are indicated by the vertical bars. The plateau was defined by four or more slopes in the scaling region deviating by no more than 5%. Plots 3(c, f) illustrate the progression of slope with embedding and the plateau

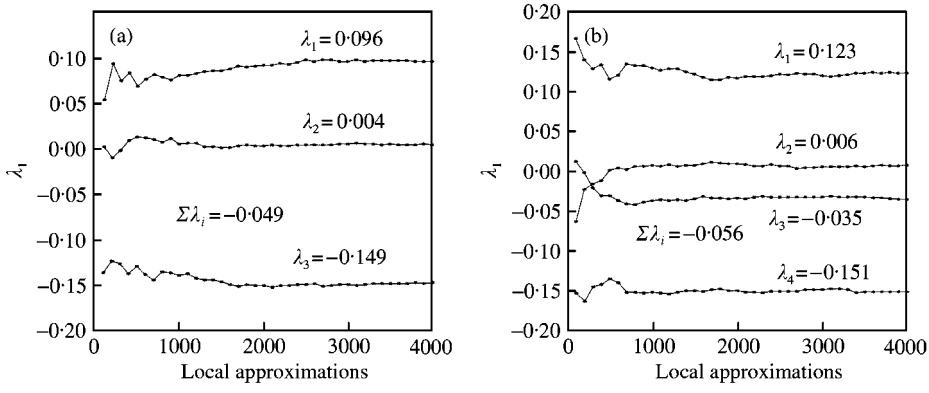

Figure 4. Lyapunov spectrum for (a) single and (b) two frequency forcing.

(average value of the last four slopes) given by the solid line. Clearly, the dynamics of the single-frequency case are occurring on a lower dimensional sub-space of d_e as $d_c = 2{\cdot}54$. Therefore, in computing the Lyapunov spectrum we expect three true exponents in the single-frequency case and four for the case of incommensurate frequency forcing. Notice that the scaling region is much more narrow for the higher-dimensional case. For a finite amount of data, the plateau is necessarily much smaller for higher-dimensional systems.

To compute the Lyapunov spectrum, Δ was chosen based on the first minimum of the average mutual information function. Following the rule of thumb given by reference [16] $\Delta = \frac{1}{2}T = 12$ time-steps for both types of forcing. The local neighborhood size, N_b, consisted of 40 and 55 points for the single- and two-frequency forced cases respectively. In both cases, the fiducial trajectory was followed for 4000 neighborhoods and results were obtained by averaging the values of the $\lambda_i(n)$ over the last 1000 iterations.

Both cases show the dominant positive exponent indicative of chaos while the sum of the exponents remains negative. In the single-frequency forced case, a clear zero exponent also appears indicating a smooth flow in time. Results in the higher-dimensional case are more difficult to interpret. If the model is to be believed, there should be two exponents associated with the flow, and hence, two zeros. Figure 4(b) shows only one zero while the other appears as a non-dominant negative exponent. This result should not be surprising. The nature of the procedure ensures that higher-dimensional systems will, in general, produce less accurate results. The application of the divergence theorem yields damping estimates of $2\zeta = 0{\cdot}049$ and $2\zeta = 0{\cdot}056$ for the single- and two-frequency forced cases respectively. Applying the Kaplan–Yorke conjecture to both cases as an additional check yields $D_L = 2{\cdot}67$ and $3{\cdot}69$. These values are indeed close to those obtained from computations of d_c, differing by roughly 4–5%.

It should be mentioned at this point that identifying spurious exponents may be extremely difficult. For this case, the spurious exponent in the single-frequency case, $\lambda_s = -0{\cdot}04$ (not shown), was ruled out by a process of elimination. The dominant positive and zero exponents were 'true' based on the fact that the data represent a chaotic flow. For the sum of the exponents to be negative (a requirement for any dissipative system), the dominant negative exponent also must be true. At least one method exists for determining the spurious measure empirically. The method, outlined in reference [19], involves computing the spectrum in reverse time. True exponents should simply flip sign while spurious ones should "do something else" according to Abarbanel. The difficulty with this technique is that it is extremely sensitive to noise.

4. COMPARISON WITH CONVENTIONAL TECHNIQUES

Having determined ζ via the divergence theorem, we now seek to make comparisons with esults obtained from two other methods, the logarithmic decrement and a parameter fitting technique. In the case of the logarithmic decrement transient data is required while the parameter fitting technique requires that the exact form of the non-linearity (stiffness term) be known.

4.1. LOGARITHMIC DECREMENT

Assuming a viscous damping model, the familiar logarithmic decrement quantifies the rate at which successive amplitudes of oscillation decay. More specifically,

$$\delta = \frac{1}{m} \ln \left(\frac{x_1}{x_{m+1}} \right), \tag{26}$$

where x_i represent the peak amplitudes of oscillation and m is the number of cycles over which the decay is being monitored. Following standard linear vibration theory [23] it may be shown that

$$\delta = \frac{2\pi\zeta}{\sqrt{1-\zeta^2}} \tag{27}$$

which, under the assumption of light damping ($\zeta \ll 1$), yields $\zeta \simeq \delta/2\pi$. The main disadvantage to the log-dec approach is that it assumes that the system in question is operating in a linear regime. Applying the technique to a non-linear system will therefore require observing a restricted subset of the dynamics.

Data for the log-dec approach were obtained by 'nudging' the cart off the hilltop and observing the free decay response at a sampling interval of $\tau_s = 0{\cdot}01s$. Trials were performed about both equilibria and the results are shown in Figure 5(a, b). Due to the asymmetry of the potential wells, initial large amplitude oscillations were ignored. In addition, damping at low amplitudes becomes dominated by dry friction which will invalidate the viscous model. Therefore, in applying equation (5) only peaks 3–12 were used. Results indicate damping values of $\zeta = 0{\cdot}023$ and $0{\cdot}024$ for the left and right wells respectively. A simple average yields

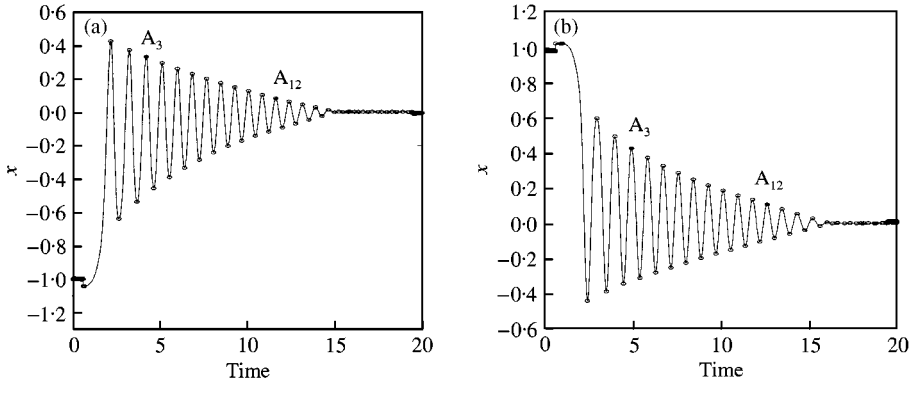

Figure 5. Free decay oscillations in (a) left ($2\zeta = 0{\cdot}048$) and (b) right ($2\zeta = 0{\cdot}046$) wells.

the log-dec estimation of $2\zeta = 0{\cdot}047$. This value is consistent with previous work [4] and reinforces the assumption of light damping.

4.2. SYSTEM IDENTIFICATION

A system identification approach (SID) was also undertaken to estimate the viscous and Coulomb damping as well as the other parameters in the Duffing oscillator experiment. The experiment was designed to replicate equations (25) which may be written in terms of the system parameters as

$$x'' + 2\zeta x' + a_0 x^3 - a_1 x = -a_2 x_b'', \tag{28}$$

with unknown parameters ζ, a_0, a_1, and a_2. By differentiating the recorded observable, x, and base acceleration, x_b, estimates of x', x'', and x_b'' were obtained. Equation (28) was fit to data by minimizing the normalized quadratic error function,

$$J = \frac{\sum_{i=1}^{N} (x_i'' - \hat{x}_i''(\zeta, a_0, a_1, a_2))^2}{\sum_{i=1}^{N} x_i''^2}, \tag{29}$$

where $\hat{x}_i''$ represents the solution to equation (28) sampled at the same times as the measured data. In other words,

$$\hat{x}'' = -2\zeta x' - a_0 x^3 + a_1 x - a_2 x_b''. \tag{30}$$

Equation (30) is linear in the parameters, which allows the parameter estimation to be cast as an overdetermined linear least-squares problem solved easily by using the SVD algorithm of section 2.1 (see Press *et al.* [24]).

The procedure was carried out by using the data described in section 3.1 (single-frequency forcing) in conjunction with the base acceleration record. Minimizing J results in $\zeta = 0{\cdot}028$, $a_0 = 0{\cdot}546$, $a_1 = 0{\cdot}533$, and $a_2 = 1{\cdot}061$. The "a" parameters are within five per cent of their designed values, and $J = 0{\cdot}034$. It should be noted that this approach also lends itself to an estimation of Coulomb damping. This is accomplished by including an additional term, $-a_3 \mathrm{sgn}(x')$, in equation (28) where a_3 is the magnitude of Coulomb damping. When Coulomb damping is included, the resulting parameters are $\zeta = 0{\cdot}022$, $a_0 = 0{\cdot}546$,

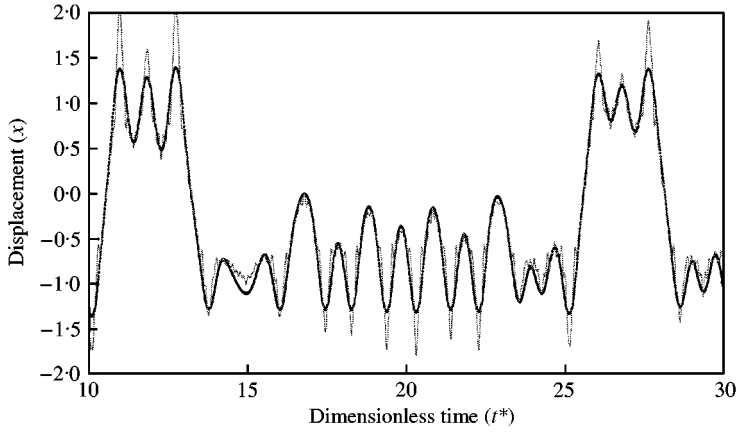

Figure 6. Experimental (···) and simulated (——) behavior of the Duffing oscillator ($t^* = 2{\cdot}4\ \pi t$).

$a_1 = 0{\cdot}533$, $a_2 = 1{\cdot}061$, and $a_3 = 0{\cdot}0054$. The small amount of added frictional damping affects the estimate of ζ only by reducing it from 2·8 per cent to 2·2 per cent. The value of the objective function did not significantly improve by the addition of the frictional damping. Figure 6 illustrates a portion of the measured data and the results of fitting equation (28) to the data.

Certain terms which depend on the shape of the track are neglected in equation (28). For small displacements these terms are negligible. However, during high amplitude (typically cross-well) oscillations the terms have a more pronounced effect as illustrated by the discrepancy between model and experiment for $|x| > 1{\cdot}3$.

5. DISCUSSION

A summary of key results for both the linear and nonlinear approaches are illustrated in Table 1. The results indicate that damping may be successfully extracted from a non-linear system, even one operating in the chaotic regime. By utilizing the invariant properties of the systems attractor, much can be learned about the way in which the system dissipates energy. The difficulty, of course, comes in obtaining reliable estimates of the Lyapunov exponents. Although algorithms are continually being improved, there currently does not exist a 'black-box' routine in which data may be processed to yield optimal results. The sheer number of parameters involved in such an estimation require a sufficient understanding of the algorithm and the effects each of the parameters may have on the outcome. Certainly, tools such as mutual information, FNN, and local dimension estimates can be exceedingly valuable in the process.

Altering the dimensionality of the system has little effect on the outcome. However, as with all measures that require an attractor reconstruction, the higher the dimensionality of the system, the less confidence one will have in the resulting measure. A good rule of thumb for data requirements is given by Nerenburg and Essex [25]. For a system of local dimension D, reliable estimates are obtained for $N_p = 2^D(D+1)^D$ points in the data set. For the amount of data used in this study, *only* systems of four or fewer dimensions may be currently analyzed from a practical point of view.

The Kaplan–Yorke conjecture provides a means of cross-checking invariant measures. However, it should be kept in mind that invariant measures are statistical quantities and should be treated as such. While no attempt has been made in this study, it may be possible to establish confidence intervals for the particular measure of interest. For example, by assuming a stationary system, several data sets may be taken and the invariant measure of choice extracted from each. Confidence intervals may then be built by using the resulting distribution. While time consuming, statistical analysis is most likely unavoidable if the techniques are to be used regularly in practice.

The last issue to address is that of noise in the signal. In this study, the signal to noise ratio is greater than 20 (less than 5% contamination). Lyapunov spectrum estimations are

TABLE 1

Experimental results

Forcing	d_c	D_L	Divergence	SID	Log-dec
None	—	—	—	—	$2\zeta = 0{\cdot}047$
Single Freq.	2·54	2·67	$2\zeta = 0{\cdot}049$	$2\zeta = 0{\cdot}056$	—
Two Freq.	3·55	3·69	$2\zeta = 0{\cdot}056$	—	—

very sensitive to noise such that a signal to noise ratio of below 10–20 may prove inadequate for quantitative results. Several non-linear 'cleaning' algorithms have been proposed which may ease this restriction. An excellent discussion of the effects of noise as well as ways of addressing the problem are discussed in reference [16]. While difficulties exist, the method nonetheless shows great promise for future work in non-linear mechanical systems.

REFERENCES

1. J. K. PINKELMAN, S. M. BATILL and M. W. KEHOE 1996 *Journal of Aircraft* **33**, 784–792. Total least-squares criteria in parameter identification for flight flutter testing.
2. D. E. NEWLAND 1993 *An Introduction to Random Vibrations, Spectral and Wavelet Analysis*. New York: Wiley, third edition.
3. K. SHIN and J. K. HAMMOND 1998 *Journal of Sound and Vibration* **218**, 389–403. The instantaneous Lyapunov exponent and its application to chaotic dynamical systems.
4. L. N. VIRGIN 2000 *Introduction to Experimental Nonlinear Dynamics: A Case Study in Mechanical Vibration*. Cambridge: Cambridge University Press.
5. J. M. NICHOLS and L. N. VIRGIN 2000 Practical evaluation of invariant measures for the chaotic response of a two-frequency excited mechanical oscillator. *Nonlinear Dynamics*, in press.
6. A. H. NAYFEH and B. BALACHANDRAN 1995 *Applied Nonlinear Dynamics: Analytical, Computational and Experimental Methods*. New York: Wiley.
7. T. KAPITANIAK 1998 *Chaos for Engineers: Theory, Applications and Control*. Berlin: Springer-Verlag.
8. A. WOLF, J. B. SWIFT, H. L. SWINNEY and J. A. VASTANO 1984 *Physica D* **16**, 285–317. Determining Lyapunov exponents from a time series.
9. F. TAKENS 1981 Detecting strange attractors in turbulence. In *Lecture notes in Mathematics*, Vol. 898, pp. 366. Berlin: Springer-Verlag.
10. A. G. DARBYSHIRE and D. S. BROOMHEAD 1996 *Physica D* **89**, 287–307. Robust estimation of tangent maps and Lyapunov spectra.
11. K. LIU 1997. *Computers and Structures* **63**, 51–59. Application of SVD in optimization of structural modal test.
12. D. S. BROOMHEAD and G. P. KING 1986 *Physica D* **20**, 217–236. Extracting qualitative dynamics from experimental data.
13. P. GRASSBERGER, T. SCHREIBER and C. SCHAFFRATH 1991 *International Journal of Bifurcation and Chaos* **1**, 521–547. Nonlinear time sequence analysis.
14. M. BANBROOK, G. USHAW and S. MCLAUGHLIN 1997 *IEEE Transactions on Signal Processing* **45**(5), 1378–1382. How to extract Lyapunov exponents from short and noisy time series.
15. TH.-M KRUEL, A. FREUND and F. W. SCHNEIDER 1990 *J. of Chem. Phys.* **93**, 416–427. The effect of interactive noise on the driven brusselator model.
16. H. KANTZ and T. SCHREIBER 1999 *Nonlinear Time Series Analysis*. Cambridge: Cambridge University Press.
17. M. B. KENNEL, R. BROWN and H. D. I. ABARBANEL 1992 *Physical Review A* **45**, 3403–3411. Determining embedding dimension for phase-space reconstruction using a geometrical construction.
18. P. BRYANT 1991 In *Proceedings of the 1st Experimental Chaos Conference*, pp. 11–23. Singapore: World Scientific. Computation of Lyapunov exponents from experimental data.
19. H. D. I. ABARBANEL 1996 *Analysis of Observed Chaotic Data*. Berlin: Springer-Verlag.
20. R. BROWN, P. BRYANT and H. D. I. ABARBANEL 1991 *Physical Review A* **43**, 2787–2806. Computing the Lyapunov spectrum of a dynamical system from an observed time series.
21. J. A. GOTTWALD, L. N. VIRGIN and E. H. DOWELL 1992 *Journal of Sound and Vibration* **158**, 447–467. Experimental mimicry of Duffing's equation.
22. H. D. I. ABARBANEL and M. KENNEL 1993 *Physical Review E* **47**, 3057–3068. Local false nearest neighbors and dynamical dimensions from observed chaotic data.
23. S. S. RAO 1995 *Mechanical Vibrations*. Reading, MA: Addison-Wesley.
24. W. H. PRESS, S. A. TEUKOLSKY, W. T. VETTERLING and B. P. FLANNERY 1992 *Numerical Recipes in C: the art of scientific computing*. Cambridge: Cambridge University Press, second edition.
25. M. A. H. NERENBERG and C. ESSEX 1990 *Physical Review A* **42**, 7065–7074. Correlation dimension and systematic geometric effects.